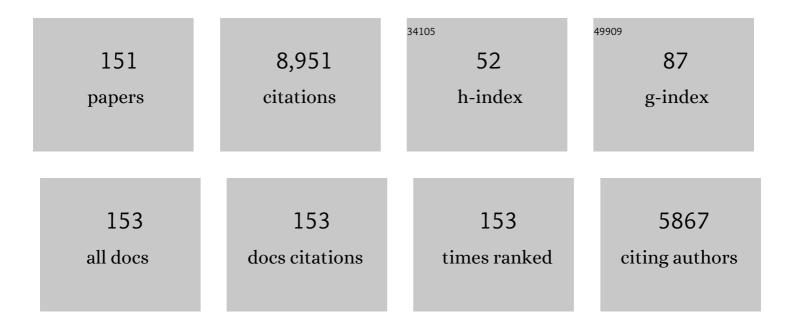
List of Publications by Year in descending order

Source: https://exaly.com/author-pdf/2356117/publications.pdf Version: 2024-02-01



#	Article	IF	CITATIONS
1	Highly efficient mesoporous MnO2 catalysts for the total toluene oxidation: Oxygen-Vacancy defect engineering and involved intermediates using in situ DRIFTS. Applied Catalysis B: Environmental, 2020, 264, 118464.	20.2	446
2	Evolution of oxygen vacancies in MnOx-CeO2 mixed oxides for soot oxidation. Applied Catalysis B: Environmental, 2018, 223, 91-102.	20.2	401
3	Size effect of Pt nanoparticles on the catalytic oxidation of toluene over Pt/CeO2 catalysts. Applied Catalysis B: Environmental, 2018, 220, 462-470.	20.2	379
4	Shape effect of Pt/CeO 2 catalysts on the catalytic oxidation of toluene. Chemical Engineering Journal, 2016, 306, 1234-1246.	12.7	280
5	Controllable synthesis of 3D hierarchical Co ₃ O ₄ nanocatalysts with various morphologies for the catalytic oxidation of toluene. Journal of Materials Chemistry A, 2018, 6, 498-509.	10.3	268
6	Conversion of fructose into 5-hydroxymethylfurfural catalyzed by recyclable sulfonic acid-functionalized metal–organic frameworks. Green Chemistry, 2014, 16, 2490-2499.	9.0	267
7	Recent Progress of Thermocatalytic and Photo/Thermocatalytic Oxidation for VOCs Purification over Manganese-based Oxide Catalysts. Environmental Science & Technology, 2021, 55, 4268-4286.	10.0	185
8	Byproducts and pathways of toluene destruction via plasma-catalysis. Journal of Molecular Catalysis A, 2011, 336, 87-93.	4.8	171
9	Effect of reduction treatment on structural properties of TiO2 supported Pt nanoparticles and their catalytic activity for formaldehyde oxidation. Journal of Materials Chemistry, 2011, 21, 9647.	6.7	157
10	In situ DRIFTS study of NO reduction by NH3 over Fe–Ce–Mn/ZSM-5 catalysts. Catalysis Today, 2011, 175, 157-163.	4.4	147
11	Adsorption of VOCs on reduced graphene oxide. Journal of Environmental Sciences, 2018, 67, 171-178.	6.1	145
12	Toluene oxidation over Co3+-rich spinel Co3O4: Evaluation of chemical and by-product species identified by in situ DRIFTS combined with PTR-TOF-MS. Journal of Hazardous Materials, 2020, 386, 121957.	12.4	141
13	Catalytic oxidation of toluene over nanorod-structured Mn–Ce mixed oxides. Catalysis Today, 2013, 216, 220-228.	4.4	134
14	Gaseous CO and toluene co-oxidation over monolithic core–shell Co ₃ O ₄ -based hetero-structured catalysts. Journal of Materials Chemistry A, 2019, 7, 16197-16210.	10.3	134
15	Toluene oxidation process and proper mechanism over Co3O4 nanotubes: Investigation through in-situ DRIFTS combined with PTR-TOF-MS and quasi in-situ XPS. Chemical Engineering Journal, 2020, 397, 125375.	12.7	134
16	Unraveling the decisive role of surface CeO2 nanoparticles in the Pt-CeO2/MnO2 hetero-catalysts for boosting toluene oxidation: Synergistic effect of surface decorated and intrinsic O-vacancies. Chemical Engineering Journal, 2021, 418, 129399.	12.7	132
17	1D-Co3O4, 2D-Co3O4, 3D-Co3O4 for catalytic oxidation of toluene. Catalysis Today, 2019, 332, 160-167.	4.4	127
18	Enhanced oxygen vacancies to improve ethyl acetate oxidation over MnOx-CeO2 catalyst derived from MOF template. Chemical Engineering Journal, 2019, 371, 78-87.	12.7	116

#	Article	IF	CITATIONS
19	Engineering Cobalt Oxide with Coexisting Cobalt Defects and Oxygen Vacancies for Enhanced Catalytic Oxidation of Toluene. ACS Catalysis, 2022, 12, 4906-4917.	11.2	116
20	Microbial Targeted Degradation Pretreatment: A Novel Approach to Preparation of Activated Carbon with Specific Hierarchical Porous Structures, High Surface Areas, and Satisfactory Toluene Adsorption Performance. Environmental Science & Technology, 2019, 53, 7632-7640.	10.0	113
21	Effects of dielectric barrier discharge plasma on the catalytic activity of Pt/CeO2 catalysts. Applied Catalysis B: Environmental, 2018, 238, 328-338.	20.2	112
22	Effect of CeO2 morphologies on toluene catalytic combustion. Catalysis Today, 2019, 332, 177-182.	4.4	111
23	The Applications of Morphology Controlled ZnO in Catalysis. Catalysts, 2016, 6, 188.	3.5	110
24	Ag supported on CeO2 with different morphologies for the catalytic oxidation of HCHO. Chemical Engineering Journal, 2018, 334, 2480-2487.	12.7	106
25	<i>In situ</i> DRIFT spectroscopy insights into the reaction mechanism of CO and toluene co-oxidation over Pt-based catalysts. Catalysis Science and Technology, 2019, 9, 4538-4551.	4.1	103
26	Plasma-catalysis of metal loaded SBA-15 for toluene removal: Comparison of continuously introduced and adsorption-discharge plasma system. Chemical Engineering Journal, 2016, 283, 276-284.	12.7	102
27	Activating Metal Oxides Nanocatalysts for Electrocatalytic Water Oxidation by Quenching-Induced Near-Surface Metal Atom Functionality. Journal of the American Chemical Society, 2021, 143, 14169-14177.	13.7	101
28	Interfacial effects in hierarchically porous α-MnO2/Mn3O4 heterostructures promote photocatalytic oxidation activity. Applied Catalysis B: Environmental, 2020, 268, 118418.	20.2	100
29	Catalytic properties of manganese oxide polyhedra with hollow and solid morphologies in toluene removal. Applied Surface Science, 2017, 405, 20-28.	6.1	97
30	Hierarchical Co 3 O 4 nanostructures in-situ grown on 3D nickel foam towards toluene oxidation. Molecular Catalysis, 2018, 454, 12-20.	2.0	95
31	MnOx supported on carbon nanotubes by different methods for the SCR of NO with NH3. Catalysis Today, 2013, 201, 115-121.	4.4	86
32	Reactivity-based industrial volatile organic compounds emission inventory and its implications for ozone control strategies in China. Atmospheric Environment, 2017, 162, 115-126.	4.1	83
33	Enhanced photocatalytic activity of rGO/TiO2 for the decomposition of formaldehyde under visible light irradiation. Journal of Environmental Sciences, 2018, 73, 138-146.	6.1	83
34	Historical industrial emissions of non-methane volatile organic compounds in China for the period of 1980–2010. Atmospheric Environment, 2014, 86, 102-112.	4.1	82
35	Elucidating the special role of strong metal–support interactions in Pt/MnO ₂ catalysts for total toluene oxidation. Nanoscale Horizons, 2019, 4, 1425-1433.	8.0	78
36	Vertically-aligned Co ₃ O ₄ arrays on Ni foam as monolithic structured catalysts for CO oxidation: effects of morphological transformation. Nanoscale, 2018, 10, 7746-7758.	5.6	76

#	Article	IF	CITATIONS
37	Design of 3-dimensionally self-assembled CeO2 hierarchical nanosphere as high efficiency catalysts for toluene oxidation. Chemical Engineering Journal, 2019, 369, 18-25.	12.7	74
38	Improved emissions inventory and VOCs speciation for industrial OFP estimation in China. Science of the Total Environment, 2020, 745, 140838.	8.0	72
39	Combination of photocatalysis downstream the non-thermal plasma reactor for oxidation of gas-phase toluene. Journal of Hazardous Materials, 2009, 171, 535-541.	12.4	71
40	Insight into the effect of manganese substitution on mesoporous hollow spinel cobalt oxides for catalytic oxidation of toluene. Journal of Colloid and Interface Science, 2021, 594, 713-726.	9.4	70
41	Amine-functionalized metal-organic frameworks for the transesterification of triglycerides. Journal of Materials Chemistry A, 2014, 2, 7205-7213.	10.3	68
42	On the performance and mechanisms of toluene removal by FeOx/SBA-15-assisted non-thermal plasma at atmospheric pressure and room temperature. Catalysis Today, 2015, 242, 274-286.	4.4	66
43	Soot oxidation via CuO doped CeO2 catalysts prepared using coprecipitation and citrate acid complex-combustion synthesis. Catalysis Today, 2010, 153, 125-132.	4.4	65
44	Leaf-like Co-ZIF-L derivatives embedded on Co2AlO4/Ni foam from hydrotalcites as monolithic catalysts for toluene abatement. Journal of Hazardous Materials, 2019, 364, 571-580.	12.4	65
45	High-efficiency non-thermal plasma-catalysis of cobalt incorporated mesoporous MCM-41 for toluene removal. Catalysis Today, 2017, 281, 527-533.	4.4	64
46	Room Temperature Catalytic Ozonation of Toluene over MnO2/Al2O3. Chinese Journal of Catalysis, 2011, 32, 904-916.	14.0	63
47	In situ FT-IR study and evaluation of toluene abatement in different plasma catalytic systems over metal oxides loaded Î ³ -Al2O3. Catalysis Communications, 2016, 84, 61-66.	3.3	63
48	Methanol plasma-catalytic oxidation over CeO2 catalysts: Effect of ceria morphology and reaction mechanism. Chemical Engineering Journal, 2019, 369, 233-244.	12.7	62
49	The simultaneous catalytic removal of VOCs and O3 in a post-plasma. Catalysis Today, 2008, 139, 43-48.	4.4	60
50	Effect of manganese oxide catalyst on the dielectric barrier discharge decomposition of toluene. Catalysis Today, 2010, 153, 176-183.	4.4	57
51	Air‣table and Dendriteâ€Free Lithium Metal Anodes Enabled by a Hybrid Interphase of C ₆₀ and Mg. Advanced Energy Materials, 2020, 10, 1903292.	19.5	57
52	Enhancing catalytic toluene oxidation over MnO2@Co3O4 by constructing a coupled interface. Chinese Journal of Catalysis, 2020, 41, 1873-1883.	14.0	57
53	Highly efficient Cu/CeO2-hollow nanospheres catalyst for the reverse water-gas shift reaction: Investigation on the role of oxygen vacancies through in situ UV-Raman and DRIFTS. Applied Surface Science, 2020, 516, 146035.	6.1	57
54	Roles of nitrogen species on nitrogen-doped CNTs supported Cu-ZrO2 system for carbon dioxide hydrogenation to methanol. Catalysis Today, 2018, 307, 212-223.	4.4	55

#	Article	IF	CITATIONS
55	Hierarchical porous carbon fabricated from cellulose-degrading fungus modified rice husks: Ultrahigh surface area and impressive improvement in toluene adsorption. Journal of Hazardous Materials, 2020, 392, 122298.	12.4	54
56	Key factors and primary modification methods of activated carbon and their application in adsorption of carbon-based gases: A review. Chemosphere, 2022, 287, 131995.	8.2	52
57	Low-temperature CO oxidation over integrated penthorum chinense-like MnCo ₂ O ₄ arrays anchored on three-dimensional Ni foam with enhanced moisture resistance. Catalysis Science and Technology, 2018, 8, 1663-1676.	4.1	48
58	Effect of calcium addition in plasma catalysis for toluene removal by Ni/ZSM-5 : Acidity/basicity, catalytic activity and reaction mechanism. Journal of Hazardous Materials, 2020, 387, 122004.	12.4	48
59	The Mechanism of Non-thermal Plasma Catalysis on Volatile Organic Compounds Removal. Catalysis Surveys From Asia, 2018, 22, 73-94.	2.6	46
60	Carbon dioxide hydrogenation to methanol over Cu/ZrO2/CNTs: effect of carbon surface chemistry. RSC Advances, 2015, 5, 45320-45330.	3.6	44
61	ZSM-5-supported V-Cu bimetallic oxide catalyst for remarkable catalytic oxidation of toluene in coal-fired flue gas. Chemical Engineering Journal, 2021, 419, 129675.	12.7	44
62	Integrated Cobalt Oxide Based Nanoarray Catalysts with Hierarchical Architectures: Inâ€Situ Raman Spectroscopy Investigation on the Carbon Monoxide Reaction Mechanism. ChemCatChem, 2018, 10, 3012-3026.	3.7	43
63	Pd-Promoted Co2NiO4 with lattice Co O Ni and interfacial Pd O activation for highly efficient methane oxidation. Applied Catalysis B: Environmental, 2021, 292, 120201.	20.2	43
64	Inhibition Effect of Phosphorus Poisoning on the Dynamics and Redox of Cu Active Sites in a Cu-SSZ-13 NH ₃ -SCR Catalyst for NO <i>_x</i> Reduction. Environmental Science & Technology, 2021, 55, 12619-12629.	10.0	43
65	Plasma-Assisted Surface Interactions of Pt/CeO2 Catalyst for Enhanced Toluene Catalytic Oxidation. Catalysts, 2019, 9, 2.	3.5	42
66	Active site structure study of Cu/Plate ZnO model catalysts for CO2 hydrogenation to methanol under the real reaction conditions. Journal of CO2 Utilization, 2020, 37, 55-64.	6.8	42
67	Synergistic effect of tunable oxygen-vacancy defects and graphene on accelerating the photothermal degradation of methanol over Co3O4/rGO nanocomposites. Chemical Engineering Journal, 2021, 425, 131658.	12.7	42
68	Enhancement of the non-thermal plasma-catalytic system with different zeolites for toluene removal. RSC Advances, 2015, 5, 72113-72120.	3.6	41
69	Allowance and allocation of industrial volatile organic compounds emission in China for year 2020 and 2030. Journal of Environmental Sciences, 2018, 69, 155-165.	6.1	40
70	Modulate the metal support interactions to optimize the surface-interface features of Pt/CeO2 catalysts for enhancing the toluene oxidation. Journal of Hazardous Materials, 2022, 424, 127505.	12.4	40
71	The effect of existence states of PdOx supported by Co3O4 nanoplatelets on catalytic oxidation of methane. Applied Surface Science, 2021, 539, 148211.	6.1	38
72	Ozone-enhanced deep catalytic oxidation of toluene over a platinum-ceria-supported BEA zeolite catalyst. Molecular Catalysis, 2018, 460, 7-15.	2.0	37

#	Article	IF	CITATIONS
73	Effect of Absorbed Sulfate Poisoning on the Performance of Catalytic Oxidation of VOCs over MnO ₂ . ACS Applied Materials & Interfaces, 2020, 12, 50566-50572.	8.0	36
74	Enhanced performance of low Pt loading amount on Pt-CeO2 catalysts prepared by adsorption method for catalytic ozonation of toluene. Applied Catalysis A: General, 2021, 625, 118342.	4.3	35
75	Controllable transformation from 1D Co-MOF-74 to 3D CoCO ₃ and Co ₃ O ₄ with ligand recovery and tunable morphologies: the assembly process and boosting VOC degradation. Journal of Materials Chemistry A, 2021, 9, 6890-6897.	10.3	34
76	Engineering Co3+-rich crystal planes on Co3O4 hexagonal nanosheets for CO and hydrocarbons oxidation with enhanced catalytic activity and water resistance. Chemical Engineering Journal, 2021, 420, 130448.	12.7	34
77	Abatement of Toluene in the Plasma-Driven Catalysis: Mechanism and Reaction Kinetics. IEEE Transactions on Plasma Science, 2011, 39, 877-882.	1.3	33
78	Transient inâ€situ DRIFTS Investigation of Catalytic Oxidation of Toluene over αâ€, γ―and βâ€MnO _{2ChemCatChem, 2020, 12, 1046-1054.}	^{1b} 3.7	33
79	Diameter-dependent catalytic activity of ceria nanorods with various aspect ratios for toluene oxidation. Chemical Engineering Journal, 2014, 256, 439-447.	12.7	32
80	Morphology-activity correlation of electrospun CeO2 for toluene catalytic combustion. Chemosphere, 2020, 247, 125860.	8.2	32
81	Chemisorbed Superoxide Species Enhanced the High Catalytic Performance of Ag/Co ₃ O ₄ Nanocubes for Soot Oxidation. ACS Applied Materials & Interfaces, 2021, 13, 21436-21449.	8.0	32
82	Plasma-Catalytic CO ₂ Hydrogenation over a Pd/ZnO Catalyst: <i>In Situ</i> Probing of Gas-Phase and Surface Reactions. Jacs Au, 2022, 2, 1800-1810.	7.9	32
83	Preparation of α-zirconium phosphate-pillared reduced graphene oxide with increased adsorption towards methylene blue. Chemical Engineering Journal, 2014, 258, 77-84.	12.7	31
84	Relationships of ozone formation sensitivity with precursors emissions, meteorology and land use types, in Guangdong-Hong Kong-Macao Greater Bay Area, China. Journal of Environmental Sciences, 2020, 94, 1-13.	6.1	31
85	Enhancement of catalytic toluene combustion over Pt–Co3O4 catalyst through in-situ metal-organic template conversion. Chemosphere, 2021, 262, 127738.	8.2	31
86	Nonthermal plasma catalysis for toluene decomposition over BaTiO3-based catalysts by Ce doping at A-sites: The role of surface-reactive oxygen species. Journal of Hazardous Materials, 2021, 405, 124156.	12.4	31
87	Mechanistic Understanding of Cu-CHA Catalyst as Sensor for Direct NH ₃ -SCR Monitoring: The Role of Cu Mobility. ACS Applied Materials & Interfaces, 2019, 11, 8097-8105.	8.0	30
88	Toluene decomposition performance and NOx by-product formation during a DBD-catalyst process. Journal of Environmental Sciences, 2015, 28, 187-194.	6.1	29
89	Low-cost photoionization sensors as detectors in GCâ€Ã—â€GC systems designed for ambient VOC measurements. Science of the Total Environment, 2019, 664, 771-779.	8.0	29
90	Highly efficient adsorptive removal of toluene using silicon-modified activated carbon with improved fire resistance. Journal of Hazardous Materials, 2021, 415, 125753.	12.4	28

#	Article	IF	CITATIONS
91	Ordered mesoporous carbons with various pore sizes: Preparation and naphthalene adsorption performance. Journal of Applied Polymer Science, 2012, 125, 3368-3375.	2.6	27
92	Effect of oxygen mobility in the lattice of Au/TiO2 on formaldehyde oxidation. Kinetics and Catalysis, 2012, 53, 239-246.	1.0	26
93	Plasma-Catalytic Oxidation of Toluene on MnxOy at Atmospheric Pressure and Room Temperature. Plasma Chemistry and Plasma Processing, 2014, 34, 1141-1156.	2.4	26
94	Catalytic oxidation of toluene over Au–Co supported on SBA-15. Materials Research Bulletin, 2015, 70, 567-572.	5.2	26
95	Insights into the effect of flue gas on synergistic elimination of toluene and NO over V2O5-MoO3(WO3)/TiO2 catalysts. Chemical Engineering Journal, 2022, 435, 134914.	12.7	26
96	Preparing hierarchical porous carbon with well-developed microporosity using alkali metal-catalyzed hydrothermal carbonization for VOCs adsorption. Chemosphere, 2022, 298, 134248.	8.2	26
97	Outstanding stability and highly efficient methane oxidation performance of palladium-embedded ultrathin mesoporous Co2MnO4 spinel catalyst. Applied Catalysis A: General, 2020, 598, 117571.	4.3	25
98	Insight into the Improvement Effect of Nitrogen Dopant in Ag/Co3O4 Nanocubes for Soot Oxidation: Experimental and Theoretical Studies. Journal of Hazardous Materials, 2021, 420, 126604.	12.4	25
99	Unravelling Phosphorus-Induced Deactivation of Pd-SSZ-13 for Passive NO _{<i>x</i>} Adsorption and CO Oxidation. ACS Catalysis, 2021, 11, 13891-13901.	11.2	25
100	Construction of Cu-Ce interface for boosting toluene oxidation: Study of Cu-Ce interaction and intermediates identified by in situ DRIFTS. Chinese Chemical Letters, 2021, 32, 3435-3439.	9.0	24
101	Plasma-Driven Catalysis Process for Toluene Abatement: Effect of Water Vapor. IEEE Transactions on Plasma Science, 2011, 39, 576-580.	1.3	23
102	A computational study on the hydrogenation of CO2 catalyzed by a tetraphos-ligated cobalt complex: monohydride vs. dihydride. Catalysis Science and Technology, 2015, 5, 1006-1013.	4.1	23
103	Adsorption-discharge plasma system for toluene decomposition over Ni-SBA catalyst: In situ observation and humidity influence study. Chemical Engineering Journal, 2020, 382, 122950.	12.7	23
104	In-Situ characterizations to investigate the nature of Co3+ coordination environment to activate surface adsorbed oxygen for methane oxidation. Applied Surface Science, 2021, 556, 149713.	6.1	23
105	The lanthanide doping effect on toluene catalytic oxidation over Pt/CeO2 catalyst. Journal of Colloid and Interface Science, 2022, 614, 33-46.	9.4	22
106	Cycled storage-discharge (CSD) plasma catalytic removal of benzene over AgMn/HZSM-5 using air as discharge gas. Catalysis Science and Technology, 2016, 6, 3788-3796.	4.1	21
107	Spectroscopic identification and catalytic relevance of NH4+ intermediates in selective NOx reduction over Cu-SSZ-13 zeolites. Chemosphere, 2020, 250, 126272.	8.2	21
108	A Hydrothermally Stable Single-Atom Catalyst of Pt Supported on High-Entropy Oxide/Al ₂ O ₃ : Structural Optimization and Enhanced Catalytic Activity. ACS Applied Materials & Interfaces, 2021, 13, 48764-48773.	8.0	21

#	Article	IF	CITATIONS
109	Boosting the electrochemical performance of hematite nanorods <i>via</i> quenching-induced metal single atom functionalization. Journal of Materials Chemistry A, 2021, 9, 3492-3499.	10.3	20
110	Surface reactive species on MnOx(0.4)-CeO2 catalysts towards soot oxidation assisted with pulse dielectric barrier discharge. Journal of Rare Earths, 2014, 32, 153-158.	4.8	19
111	Catalytic Performance of Toluene Combustion over Pt Nanoparticles Supported on Pore-Modified Macro-Meso-Microporous Zeolite Foam. Nanomaterials, 2020, 10, 30.	4.1	19
112	Pt/MnOx for toluene mineralization via ozonation catalysis at low temperature: SMSI optimization of surface oxygen species. Chemosphere, 2022, 286, 131754.	8.2	18
113	Reverse water-gas shift in a packed bed DBD reactor: Investigation of metal-support interface towards a better understanding of plasma catalysis. Applied Catalysis A: General, 2020, 591, 117407.	4.3	17
114	In-situ atmosphere thermal pyrolysis of spindle-like Ce(OH)CO3 to fabricate Pt/CeO2 catalysts: Enhancing Pt–O–Ce bond intensity and boosting toluene degradation. Chemosphere, 2021, 279, 130658.	8.2	17
115	A dual plasmonic core—shell Pt/[TiN@TiO2] catalyst for enhanced photothermal synergistic catalytic activity of VOCs abatement. Nano Research, 2022, 15, 7071-7080.	10.4	17
116	Dendrite-free and air-stable lithium metal batteries enabled by electroless plating with aluminum fluoride. Journal of Materials Chemistry A, 2020, 8, 9218-9227.	10.3	16
117	A high-performance and stable Cu/Beta for adsorption-catalytic oxidation in-situ destruction of low concentration toluene. Science of the Total Environment, 2022, 833, 155288.	8.0	16
118	Carbonyls from commercial, canteen and residential cooking activities as crucial components of VOC emissions in China. Science of the Total Environment, 2022, 846, 157317.	8.0	16
119	Removal of toluene in adsorption–discharge plasma systems over a nickel modified SBA-15 catalyst. RSC Advances, 2016, 6, 104104-104111.	3.6	15
120	Macroporous Ni foam-supported Co3O4 nanobrush and nanomace hybrid arrays for high-efficiency CO oxidation. Journal of Environmental Sciences, 2019, 75, 136-144.	6.1	15
121	CeO2-Supported Pt Catalysts Derived from MOFs by Two Pyrolysis Strategies to Improve the Oxygen Activation Ability. Nanomaterials, 2020, 10, 983.	4.1	15
122	Cu-VWT Catalysts for Synergistic Elimination of NO _{<i>x</i>} and Volatile Organic Compounds from Coal-Fired Flue Gas. Environmental Science & Technology, 2022, 56, 10095-10104.	10.0	15
123	Effect of oxygen vacancy on the oxidation of toluene by ozone over Ag-Ce catalysts at low temperature. Applied Surface Science, 2022, 601, 154237.	6.1	15
124	Influence of Alkali Metals with Different Ionic Radius Doping into Ce0.7Zr0.3O2 on the Active Oxygen. Catalysis Letters, 2014, 144, 685-690.	2.6	14
125	Recent Understanding of Low-Temperature Copper Dynamics in Cu-Chabazite NH3-SCR Catalysts. Catalysts, 2021, 11, 52.	3.5	14
126	Performance of Toluene Removal in a Nonthermal Plasma Catalysis System over Flake-Like HZSM-5 Zeolite with Tunable Pore Size and Evaluation of Its Byproducts. Nanomaterials, 2019, 9, 290.	4.1	13

#	Article	IF	CITATIONS
127	Macroscopic Hexagonal Co ₃ O ₄ Tubes Derived from Controllable Two-Dimensional Metal-Organic Layer Single Crystals: Formation Mechanism and Catalytic Activity. Inorganic Chemistry, 2020, 59, 3062-3071.	4.0	13
128	Micro-mesoporous carbon fabricated by Phanerochaete chrysosporium pretreatment coupling with chemical activation: Promoting effect and toluene adsorption performance. Journal of Environmental Chemical Engineering, 2021, 9, 105054.	6.7	13
129	Low Pt Loading High Catalytic Performance of PtFeNi/Carbon Nanotubes Catalysts for CO Preferential Oxidation in Excess Hydrogen I: Promotion Effects of Fe and/or Ni. Catalysis Letters, 2012, 142, 975-983.	2.6	12
130	Effects of Zr substitution on soot combustion over cubic fluorite-structured nanoceria: Soot-ceria contact and interfacial oxygen evolution. Journal of Environmental Sciences, 2021, 101, 293-303.	6.1	12
131	Quenching-induced surface modulation of perovskite oxides to boost catalytic oxidation activity. Journal of Hazardous Materials, 2022, 433, 128765.	12.4	12
132	The Study of Reverse Water Gas Shift Reaction Activity over Different Interfaces: The Design of Cu-Plate ZnO Model Catalysts. Catalysts, 2020, 10, 533.	3.5	11
133	Volatile organic compounds concentration profiles and control strategy in container manufacturing industry: Case studies in China. Journal of Environmental Sciences, 2021, 104, 296-306.	6.1	11
134	Investigation into the roles of different oxygen species in toluene oxidation over manganese-supported platinum catalysts. Molecular Catalysis, 2021, 507, 111569.	2.0	10
135	3D geometric modeling analysis of contact probability effect in carbon black oxidation over MnOx-CeO2 catalysts. Chemical Engineering Journal, 2020, 398, 125448.	12.7	10
136	Emission characteristics and ozone formation potentials of VOCs from ultra-low-emission waterborne automotive painting. Chemosphere, 2022, 305, 135469.	8.2	10
137	Synergistic Effect of a Carbon Black Supported PtAg Nonâ€Alloy Bimetal Nanocatalyst for CO Preferential Oxidation in Excess Hydrogen. ChemCatChem, 2012, 4, 1960-1967.	3.7	9
138	The graphitic carbon strengthened synergetic effect between Pt and FeNi in CO preferential oxidation in excess hydrogen at low temperature. Catalysis Science and Technology, 2016, 6, 98-106.	4.1	9
139	Interfaces in MOF-Derived CeO2–MnOX Composites as High-Activity Catalysts for Toluene Oxidation: Monolayer Dispersion Threshold. Catalysts, 2020, 10, 681.	3.5	9
140	Solar photocatalytic ozonation of emerging contaminants detected in municipal wastewater treatment plant effluents by magnetic MWCNTs/TiO ₂ nanocomposites. RSC Advances, 2015, 5, 96896-96904.	3.6	8
141	Effect of plasma on catalytic conversion of CO ₂ with hydrogen over Pd/ZnO in a dielectric barrier discharge reactor. Journal Physics D: Applied Physics, 2019, 52, 244001.	2.8	8
142	Preparation of porous carbon based on partially degraded raw biomass by Trichoderma viride to optimize its toluene adsorption performance. Environmental Science and Pollution Research, 2021, 28, 46186-46195.	5.3	8
143	Synergistic catalytic ozonation of toluene with manganese and cerium varies at low temperature. Chinese Chemical Letters, 2022, 33, 2726-2730.	9.0	7
144	Unraveling specific role of carbon matrix over Pd/quasi-Ce-MOF facilitating toluene enhanced degradation. Journal of Rare Earths, 2022, 40, 1751-1762.	4.8	7

#	Article	IF	CITATIONS
145	Tuning the local electronic structure of SrTiO3 catalysts to boost plasma-catalytic interfacial synergy. Journal of Hazardous Materials, 2022, 428, 128172.	12.4	7
146	Porous stainless-steel fibers supported CuCeFeOx/Zeolite catalysts for the enhanced CO oxidation: Experimental and kinetic studies. Chemosphere, 2022, 291, 132778.	8.2	6
147	Challenges, mitigation strategies and perspectives in development of Li metal anode. Nano Select, 2020, 1, 622-638.	3.7	4
148	Experimental and computational investigation on the organic acid modification of porous carbon for toluene adsorption under humid conditions. Chemical Engineering Journal, 2022, 450, 138070.	12.7	3
149	Synthesis of Hydrophobic Mesoporous Material MFS and Its Adsorption Properties of Water Vapor. Journal of Spectroscopy, 2014, 2014, 1-7.	1.3	2
150	Performance of a Novel Hydrophobic Mesoporous Material for High Temperature Catalytic Oxidation of Naphthalene. Journal of Spectroscopy, 2014, 2014, 1-7.	1.3	1
151	REMOVAL OF METHYLENE BLUE BY AN AQUEOUS SUSPENSION OF NANO-SIZED TIO2 CONTAINING DIFFERENT SALTS. Environmental Engineering and Management Journal, 2015, 14, 2865-2870.	0.6	0